The Pore of the Leaf Cavity of *Azolla* : Morphology, Cytochemistry and Possible Functions

PASCAL VEYS, LUC WATERKEYN, ANDRE LEJEUNE* and
CHARLES VAN HOVE
Laboratory of Plant Biology, Faculty of Sciences, Catholic University of Louvain, Place Croix du Sud 5 bte 14, B-1348 Louvain-la-Neuve, Belgium, Tel. +32-10-473403, Fax. +32-10-473471, E-mail. Lejeune@bota.ucl.ac.be

Abstract

Light and transmission electron microscopy were used to describe the leaf cavity pore of *Azolla*. The morphological analysis of the pore revealed that it remains open during leaf development as well as in mature leaves. As it seems that there is no obstruction of the pore by any mucilage, gas exchanges between the atmosphere and the inner gaseous compartment of the leaf cavity are likely to occur. The pore, which is cone-shaped and protrudes into the leaf cavity, is limited by two epidermal cell layers. The cells lining the inside of the pore become teat-shaped during pore morphogenesis. Ultrastructural study of these cells showed the presence of a large number of organelles, paramural bodies and 'wart-like' projections at their cell wall surface, suggesting a secretory role. Cytochemical stains showed that these projections are made up of pectin, callose and protein. The role of the pore as well as the possible functions of the teat-cells and their projections are discussed.

Keywords: *Azolla*, *Anabaena azollae*, leaf pore, pectin, callose, cell wall projections, gas exchanges

*The author to whom correspondence should be sent.

1. Introduction

The small aquatic fern *Azolla* realizes a symbiosis with a nitrogen-fixing cyanobacterium initially described as *Anabaena azollae* Strasb. (Strasburger, 1873) even if some authors classify it among genus *Nostoc* (e.g. Meeks et al.,
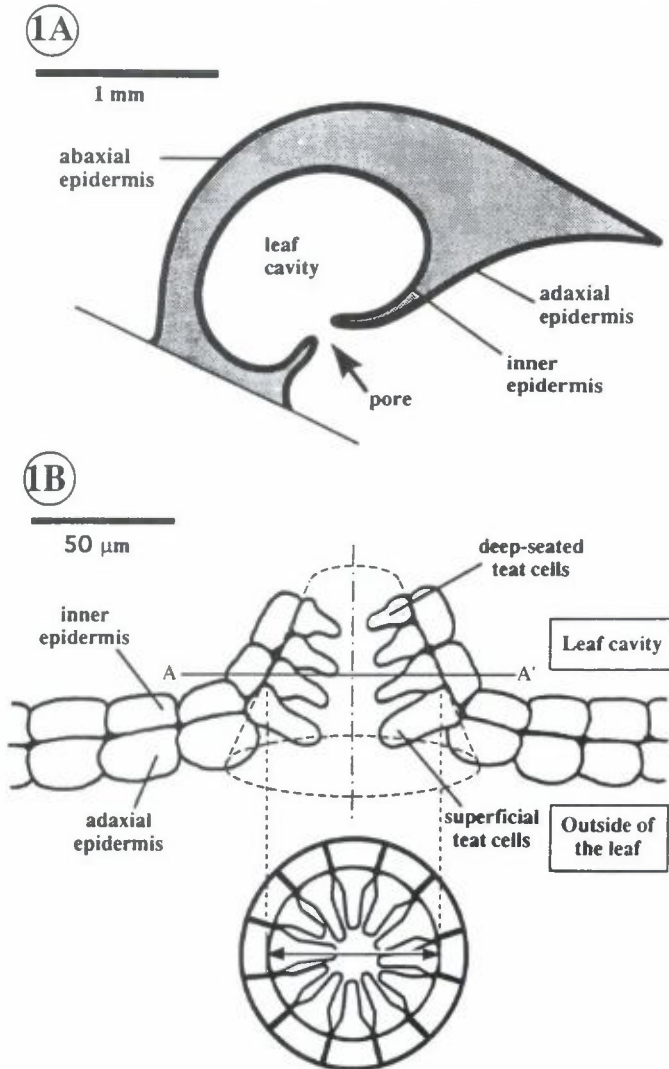

Figure 1.   A. Schematic representation of the *Azolla* upper leaf lobe showing the different epidermis and the pore region. B. Schematic representation of the *Azolla* leaf cavity pore based on longitudinal and cross sections as in Figs. 3 and 4. Upper diagram: longitudinal axial section of a typical pore. Lower diagram: cross section of the pore along the A-A' axis drawn on the upper diagram. Double arrow indicates the mean diameter of a pore, as measured in the present study.
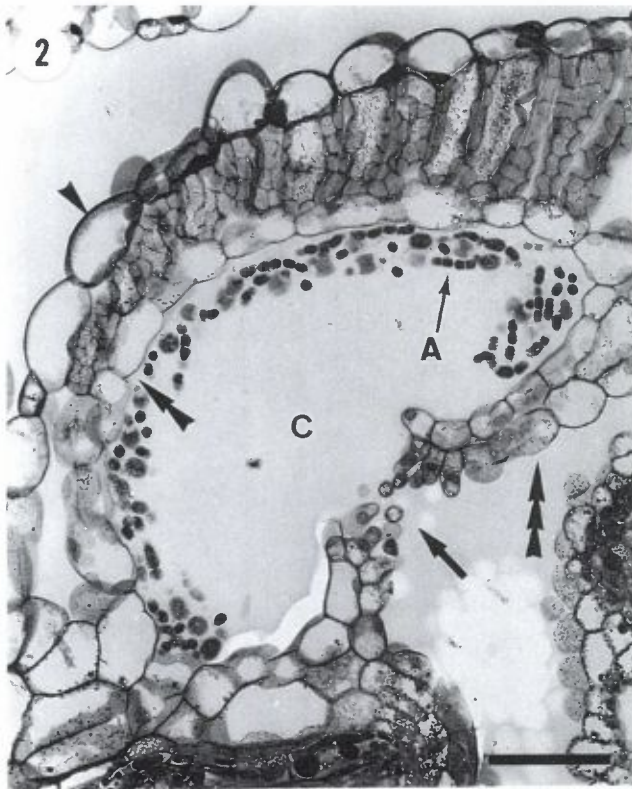
Figure 2. Longitudinal axial section of the mature upper leaf lobe showing the leaf cavity (C) with the *Anabaena* (A), and the cavity pore (arrow). The different epidermis are indicated: the abaxial epidermis (arrowhead), the inner epidermis (double arrowhead) and the adaxial epidermis (triple arrowhead). Bar = 50 μm. Light micrograph.

1988) or genus *Trichormus* (e.g. Komárek and Anagnostidis, 1989). The *Azolla* leaves are bilobed: a thin and nearly achlorophyllous lower lobe rests on the water surface (Strasburger, 1873) while the aerial chlorophyllous upper lobe (Fig. 1A) contains a cavity lined by an inner epidermis (Konar and Kapoor, 1972). *Anabaena* as well as different bacteria, some probably belonging to the genus *Arthrobacter* (Nierzwicki-Bauer and Aulfinger, 1991), are confined to the cavity and localized at its periphery within a mucilaginous matrix (Schaede, 1947) surrounding a gaseous central region (Peters and Meeks, 1989; Uheda et al., 1995). At the adaxial surface, the leaf cavity is separated from the outside by a velum, consisting of a double layer of epidermal cells, presenting a small pore (Strasburger, 1873).
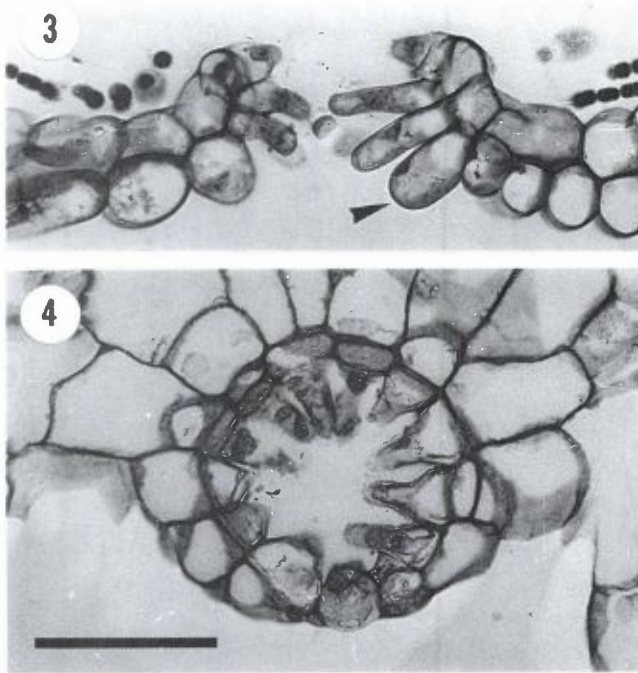
Figures 3–4. Longitudinal (Fig. 3) and cross sections (Fig. 4) through the mature pore
showing the teat-cells. Fig. 3 shows superficial teat-cells (arrowhead)
which are larger in volume than other teat-cells. Bar = 50 µm. Light
micrographs.

This pore has repeatedly been mentioned in literature. Strasburger (1873)
and Demalsy (1953), working respectively on mature leaves of *A. filiculoides*
and *A. nilotica*, described an open leaf cavity pore. An open pore was also
reported in the ontogenetical studies of Rao (1935) and Konar and Kapoor
(1972) on *A. pinnata*. In contrast, several works described a closure of the pore
at the end of leaf ontogenesis in *A. filiculoides* (Smith, 1955) and *A.
caroliniana* (Peters et al., 1978), resulting in the imprisonment of *Anabaena*
within the cavity. In 1981, the closure of the cavity pore in *A. caroliniana* was
again indicated by Calvert and Peters, and more recently, Becking (1987),
working on *A. filiculoides*, supported the report of Smith (1955).

The question as to whether the leaf cavity pore of *Azolla* remains open or
not is still unsolved. This does not seem to be due to structural differences
existing between *Azolla* species since, depending on authors, the pore of *A.*
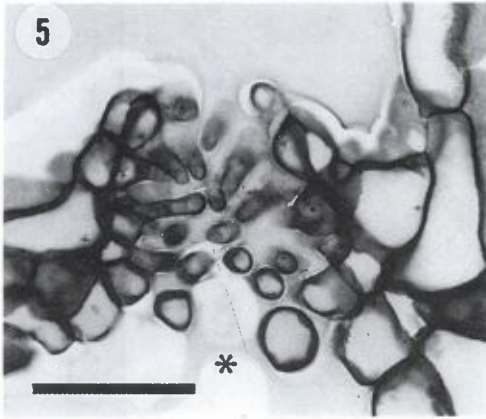
Figure 5. Longitudinal section through a fully differentiated pore showing the orientation of the teat-cells towards the pore axis and the outside of the cavity (*) as well as the complexity of the pore. Bar = 50 μm. Light micrograph.

Figure 6. Longitudinal axial section of an upper foliar primordium (developmental stage intermediate between the two developing leaves shown in Fig. 7). The margins of the bi-layered fold limiting the developing cavity are indicated with arrowheads. Bar = 20 μm. Light micrograph.
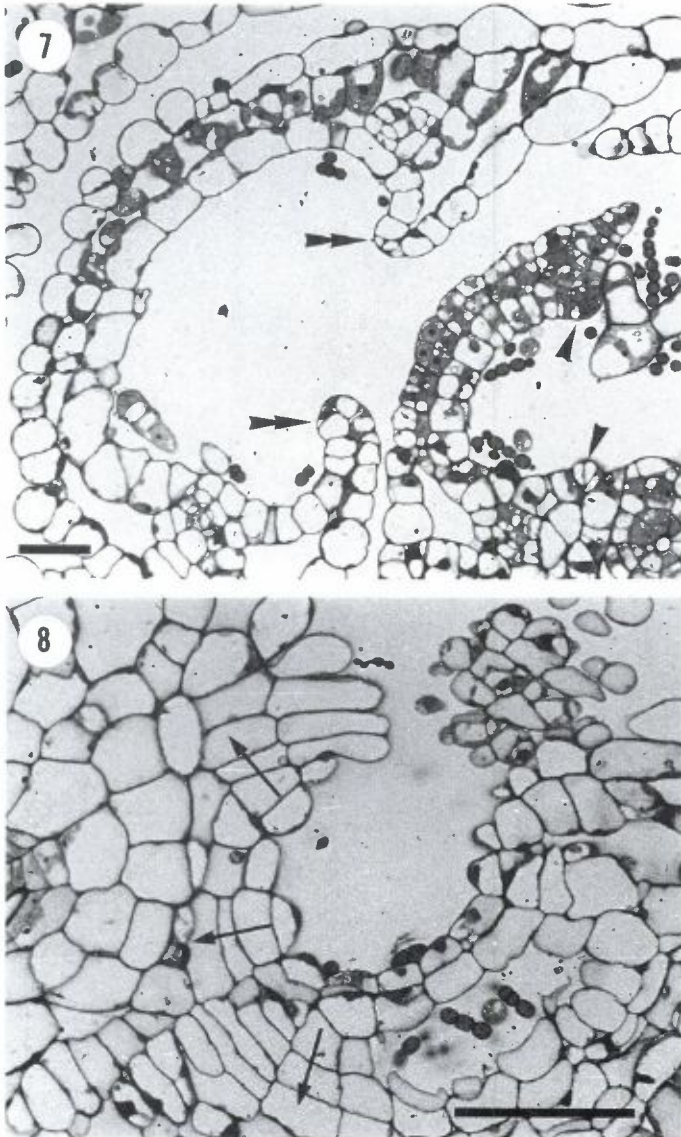
Figure 7. Longitudinal axial section of developing upper leaf lobes. The upper foliar
          primordium on the right shows the very first formation stage of the concentric
          bi-layered fold arising from the meristematic epidermal cells of the adaxial
          surface (arrowheads). The very young upper leaf lobe on the left shows the
          invagination of the fold borders (double arrowheads). Bar = 20 μm. Light
          micrograph.
Figure 8. Tangential cross section through a pore showing the radial files of cells
          (arrows) which have arisen from divisions of the meristematic cells limiting the
          developing pore (same developmental stage as shown in Fig. 9). Bar = 50 μm.
          Light micrograph.
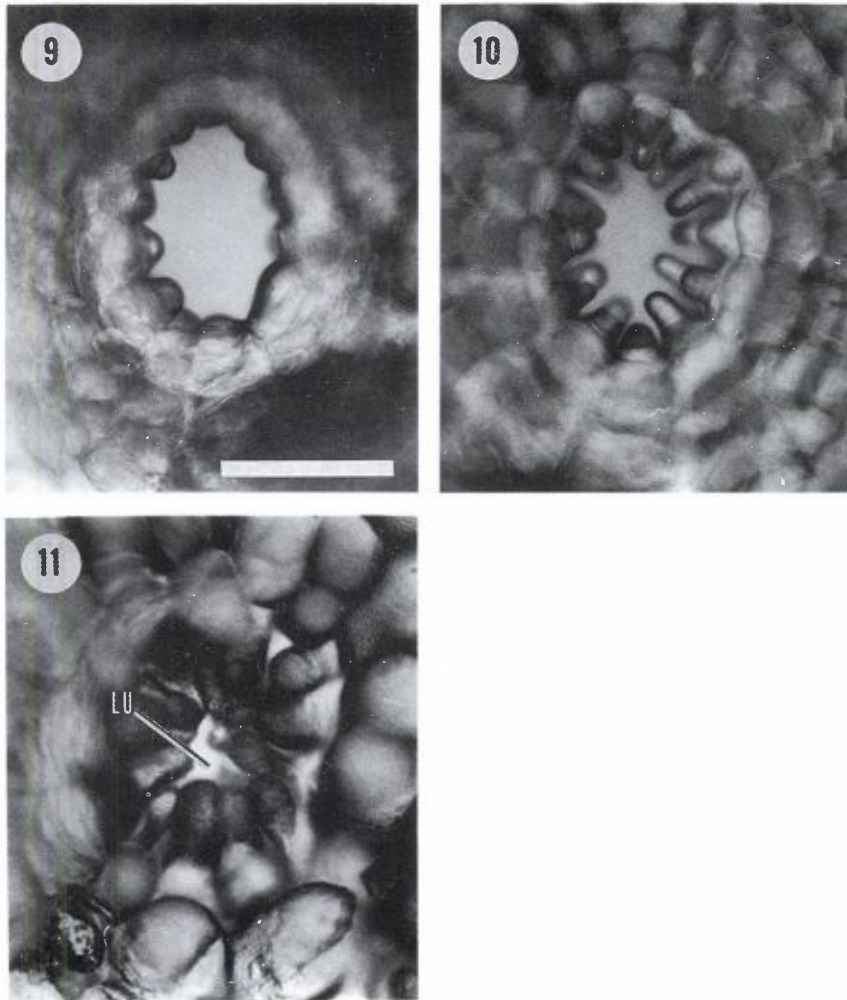
Figures 9–11. Leaf cavity pores observed on fresh leaves at different stages of development: very young (Fig. 9), young (Fig. 10) and mature leaf (Fig. 11) showing the lumen (LU). Bar = 50 μm. Light micrographs.

filiculoides was viewed as open (Strasburger, 1873) or closed (Smith, 1955; Becking, 1987). Knowing if the pore is actually open in mature leaves of *Azolla* is however essential to determine whether the symbionts are in direct contact with the external environment. If it is the case, the question of how possible exchanges may be controlled through the pore has to be addressed. This information will undoubtedly contribute in improving our understanding of the symbiosis.

Figure 12.   Longitudinal axial section through a teat-cell. The cell is highly vacuolated
and the nucleus (N) has a median position. Bar = 10 μm. Transmission electron
micrograph.

The aim of the present study was to describe precisely the morphology and
the ontogenesis of the pore; this has been carried out for three
phylogenetically distant *Azolla* species (Van Coppenolle et al., 1993)
including *A. filiculoides* for which contradictory reports exist in the literature.
Using morphological and cytochemical methods, this paper also contributes in
bringing first insights on the possible role of the pore within the symbiosis.

Figure 13. Cytoplasmic portion of a teat-cell with a Golgi apparatus located near the cell wall (CW). Secretion vesicles are visible (arrows). Note the presence of dilated Golgi cisternae (arrowheads) with an electron transparent content that seems to be limited by a double membrane. Bar = 100 nm. Transmission electron micrograph.

2. Materials and Methods

Plant material

Three *Azolla* species were used. Two strains were from the collection of the
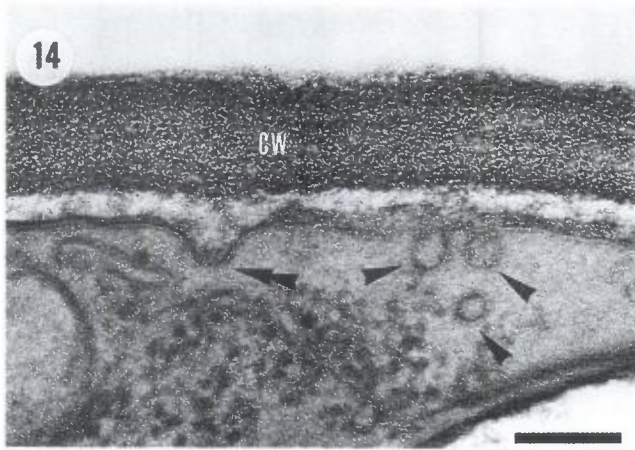
Figure 14.   Secretion vesicles (arrowheads) in close contact with the plasmalemma. A
              vesicle (double arrowhead) that may be fusing with the plasmalemma is also
              visible (cell wall = CW). Bar = 100 nm. Transmission electron micrograph.

Laboratory of Plant Biology, Catholic University of Louvain: *A. filiculoides*
(ADUL-173FI) and *A. pinnata* var. *pinnata* (ADUL-136PP) (Van Hove et al.,
1987). Culture conditions were as described by Van Hove et al. (1987). In
addition, permanent preparations of *A. nilotica* made by Demalsy (1953) were
also observed.

Light microscopy (LM)

Fronds were fixed in 70% ethanol for 24 h, then in 80% ethanol for 6–8 h and
embedded in a hydroxyethylmethacrylate resin (Technovit 7100, Kulzer,
Germany). Sections of 3–6 μm were cut with a glass knife. In addition semi-
thin sections of 2 μm were obtained from fronds prepared for transmission
electron microscopy (see below). These sections were cut with a diamond knife.
All the sections were stained with 0.1% Toluidine blue in 1% $Na_2B_4O_7$. The
sections were mounted in immersion oil.

Freshly excised upper leaf lobes were also directly observed using a bright
field light microscope. They were placed on their dorsal face on a piece of wet
filter paper so that their adaxial face, showing the pore region, was readily
observable.

Observations were made using a light microscope Polyvar (Reichert-Jung).
Micrographs were recorded on Kodak T-MAX 100 (Iso 100/21°) and Ektachrome
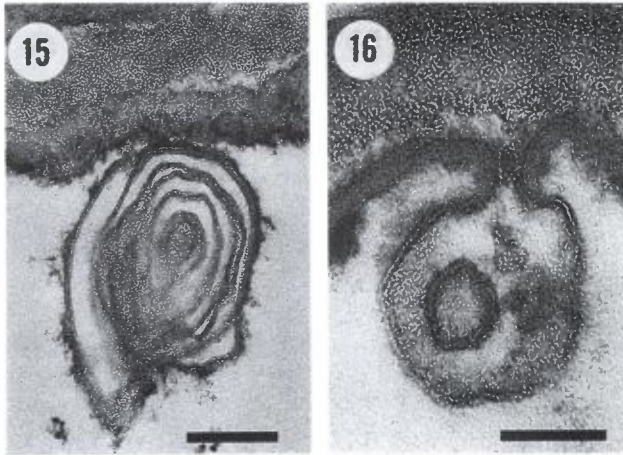64T (Iso 64/19°) films.

Figure 15. Convoluted membrane accumulations. Such structures are often observed in the vacuole close to the tonoplast of the teat-cells. Their origin could be explained by the transfer of excess membranes to the vacuole by means of plasmalemmasomes (Fig. 16). Bar = 200 nm. Transmission electron micrograph.
Figure 16. Plasmalemmasome protruding into the vacuole of a teat-cell. Bar = 100 nm. Transmission electron micrograph.

Transmission electron microscopy (TEM)

Two fixation procedures were used in this study: (i) a double fixation with glutaraldehyde-osmium tetroxide and (ii) a combined glutaraldehyde-paraformaldehyde-osmium tetroxide fixation. Procedure (i) was carried out essentially as described by Roland and Vian (1991). *Azolla* fronds were prefixed for 48 h at 4°C in a solution of 2.5% glutaraldehyde and 5 mM $CaCl_2$ in 0.05 M cacodylate buffer (pH 6.8). Fixation procedure (ii) was modified from Calvert et al. (1985) and Roland and Vian (1991) as follows: fronds were prefixed for 2 h at 20°C in a solution of 2.5% glutaraldehyde, 3.7% paraformaldehyde in the same buffer as used in procedure (i). Samples from both fixation procedures were postfixed for 30 min at 0°C in 2% OsO_4 in 0.1 M cacodylate buffer (pH 7.2).

The samples were dehydrated in a graded ethanol series and embedded in a low viscosity resin (Spurr, 1969). Resin blocks were trimmed and sectioned with a diamond knife. Ultra-thin sections of 70–90 nm were mounted on 300-mesh HH copper grids and stained using 2% uranyl acetate for 3 min followed by lead citrate for 3 min (Reynolds, 1963). Sections were observed using a Philips EM 301 transmission electron microscope operating at 60 kV. Electron micrographs were recorded on Kodak 4489 ESTAR Thick Base electron microscope film.
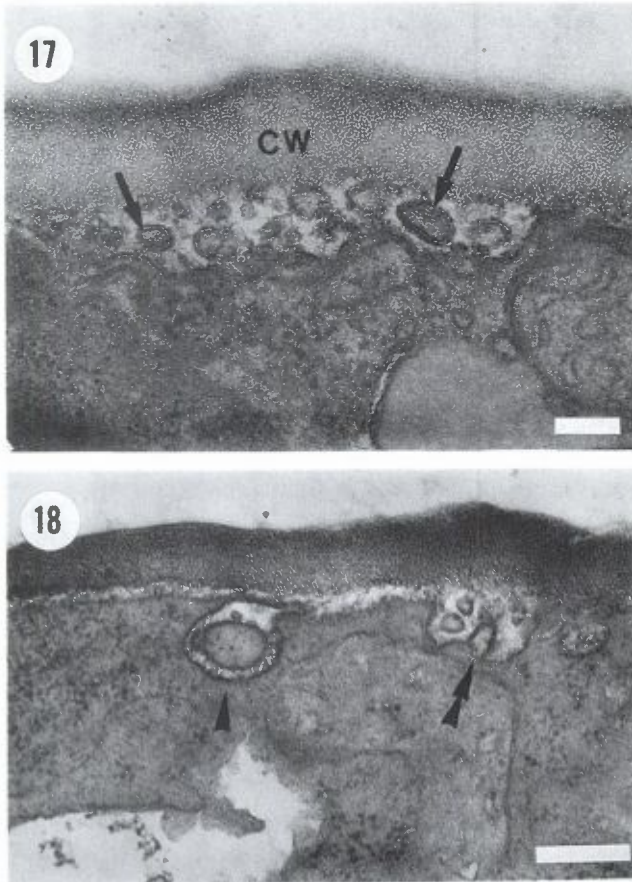
Figure 17.   Paramural body containing vesicles (arrows) filled with electron dense
             material in the periplasm next to the cell wall (CW).   Bar = 100 nm.
             Transmission electron micrograph.
Figure 18.   Two types of membranous structures observed in the periplasmic region of
             teat-cells. A multivesicular body (arrowhead) and a paramural body (double
             arrowhead) are indicated. Bar = 200 nm. Transmission electron micrograph.

Cytochemical stainings

Aqueous Ruthenium Red (1% w/v) for pectin (Jensen, 1962) was applied to
Technovit 7100 embedded sections. Hydroxylamine/ferric chloride for
esterified pectin (Reeve, 1959) was applied to fronds fixed in 70% ethanol.
Alcian blue for acidic polysaccharides was applied as described by Jeffree et
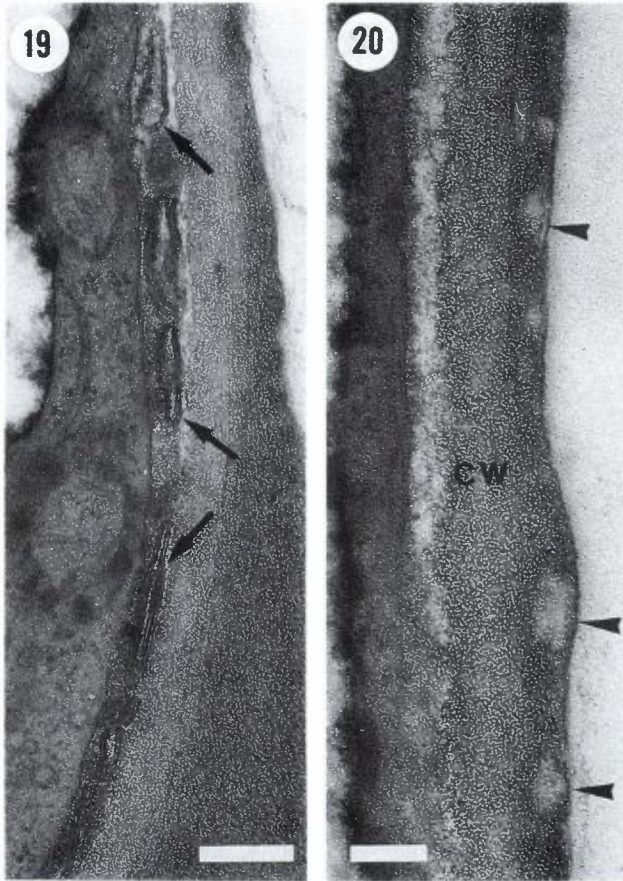
Figure 19. Paramural body with elongated and flattened vesicles (arrows) in the periplasm. Such structures are frequently observed in the often enlarged portion of the periplasm at the basal part of teat-cells. Bar = 200 nm. Transmission electron micrograph.

Figure 20. Lomasomes (arrowheads) embedded in cell wall (CW) material. The uppermost structure in the figure shows the membrane that still limits it. Bar = 100 nm. Transmission electron micrograph.

al. (1989) to fronds macerated in EDTA (Letham, 1960). The metachromatic dye Toluidine blue for acidic polysaccharides was applied to sections (see above). Calcofluor white (0.01% w/v) for cellulose, and aniline blue (0.1% w/v of water soluble aniline blue, pH adjusted to 9 with 30% NH_4OH) for callose were applied to fresh and EDTA-macerated leaves and viewed by fluorescence under UV excitation ($\lambda = 365$ nm). Aqueous resorcine blue (0.01% w/v) for
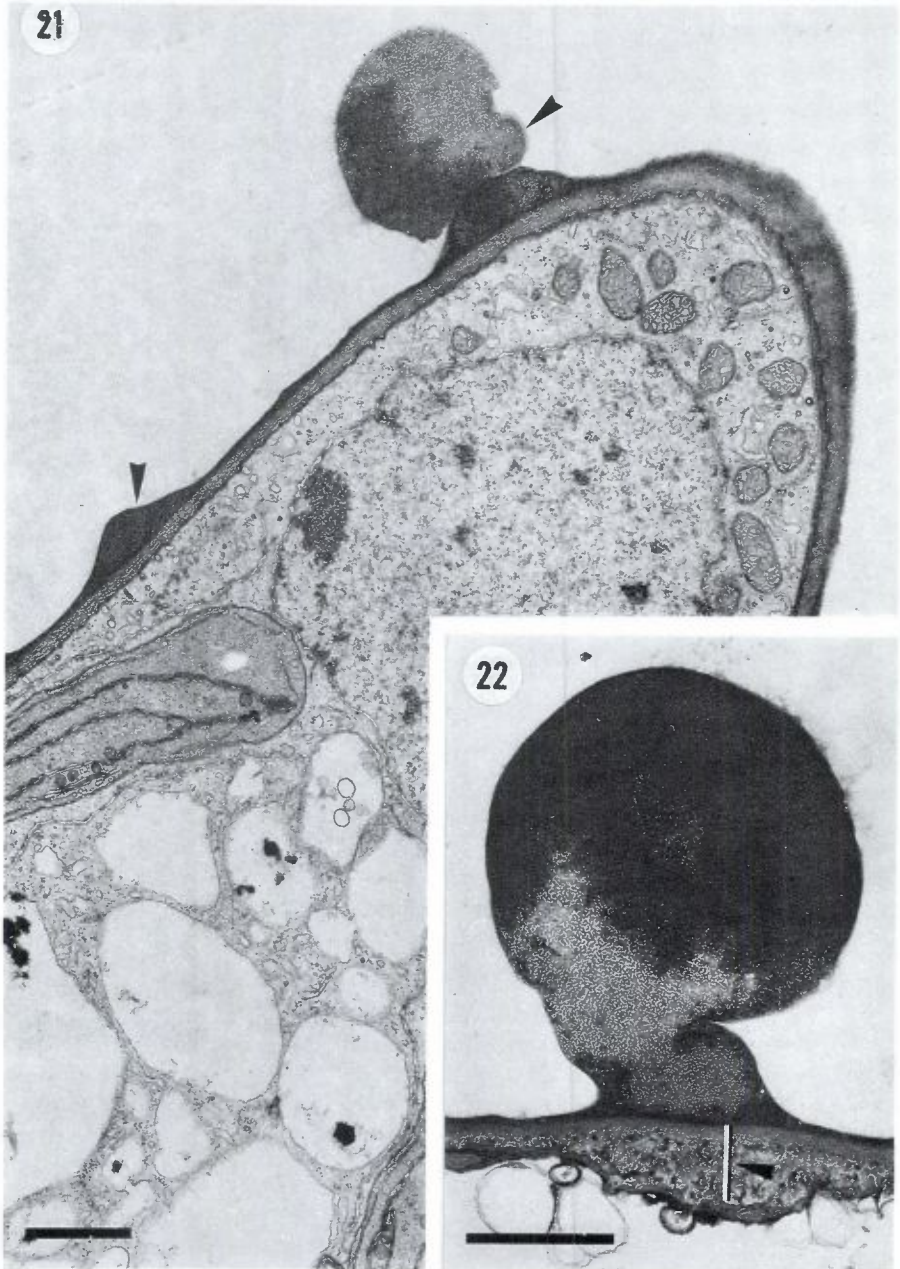
Figure 21.   Differentiated teat-cell presenting cell wall projections (arrowheads) on its
             surface. Note that it is an oblique section through the basal halfpart of a teat-
             cell. Bar = 1 μm. Transmission electron micrograph.
Figure 22.   Cell wall projection on the surface of a teat-cell. Note the thickened cell wall
             at the base of the projection (arrowhead). Bar = 1 μm. Transmission electron
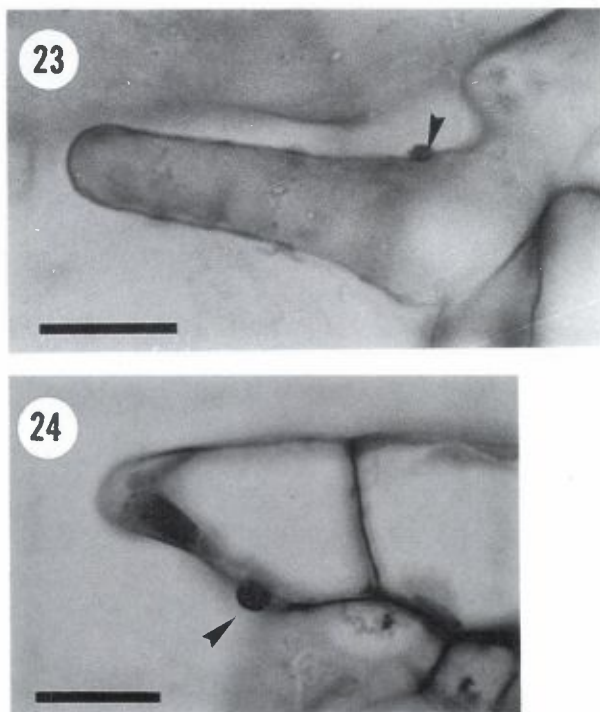   micrograph.

Figure 23. Cell wall projection (arrowhead) on the surface of a teat-cell stained by Ruthenium Red. Bar = 10 μm. Light micrograph.

Figure 24. Cell wall projection (arrowhead) stained by Toluidine blue. Bar = 10 μm. Light micrograph.

callose was applied to fresh leaves. Phosphine 3R (Popper, 1944) and Sudan Black B (Jensen, 1962) for lipids were used respectively on fresh and ethanol fixed fronds. Phosphine 3R preparations were observed by fluorescence ($\lambda = 365$ nm) under blue excitation. Coomassie Brilliant Blue R for protein (Fisher, 1968) was applied to Technovit 7100 embedded sections and EDTA-macerated leaves. Unstained preparations were also observed for autofluorescence. Nomarski interferential contrast was used to ascertain the presence of projections when staining methods failed to reveal them.

3. Results

Morphology of the differentiated pore

The morphology of the pore of mature leaves of *A. filiculoides* was
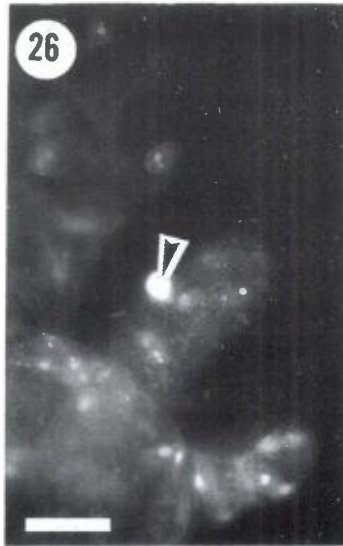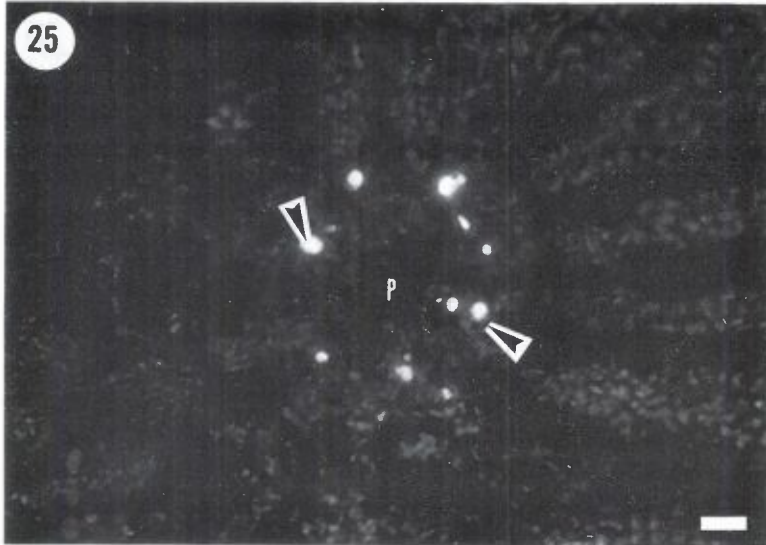
Figures 25–26. Cell wall projections (arrowheads) stained by Aniline blue under UV
                     excitation. Fig. 25 shows a fresh leaf preparation presenting the pore (P)
                     region. Note that projections are only found on teat-cells. Fig. 26 shows a
                     EDTA-macerated leaf preparation. Bars = 10 μm. Light micrographs.

investigated first. Longitudinal axial sections through the upper leaf lobes
indicate that the pore is located at the base of their adaxial surface and
bounded by two cell layers (Figs. 1A, 2, 3). One cell layer, lining the inside of

Figure 27.   Cell wall projection (arrowhead) stained by Coomassie Brilliant Blue R, after
EDTA maceration, indicating the presence of proteins. Bar = 10 μm. Light
micrograph.

the pore, is made up of teat-shaped trichomes differentiated from the adaxial
epidermis. The second cell layer corresponds to the inner epidermis lining the
cavity side of the pore (Fig. 1B). Longitudinal sections show 3–4 tiers of teat-
cells per pore, the superficial ones being larger than the deep-seated ones (Fig.
3). Cross sections (i.e. perpendicular to the pore axis) at different levels show
that the pore is circular, or occasionally slightly elliptic, and lined by about
ten teat-cells per tier, joined side by side at their basal portion (Fig. 4). The
teat-cells point towards the centre of the pore and slightly towards the outside
of the leaf cavity (Fig. 5). Based on light microscope observations of cross and
longitudinal serial sections through the pore, the schematic representation
shown in Fig. 1B was prepared. The pore is a truncated cone protruding towards
the leaf cavity (Figs. 1B, 2, 3). The mean diameter of this cone, i.e. measured
at the bases of two diametrically opposed teat-cells (Fig. 1B), is on the
average 80 μm. The pore is partially obstructed by the protruding teat-cells,
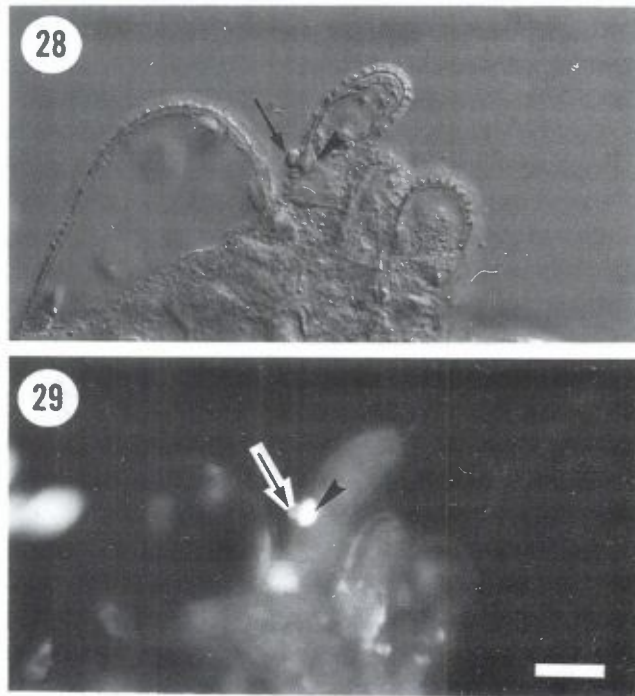
Figures 28–29. Callosic thickening (arrowheads) under a cell wall projection (arrows)
                after EDTA-maceration. Figs. 28 and 29 are the same structure, Fig. 28 is
                seen by interferential contrast and Fig. 29 is stained by Aniline blue under
                UV excitation. Bar = 10 μm. Light micrographs.

which are sometimes so elongated that their apices can overlap; physical
contact was nevertheless never observed between teat-cell apices. Sometimes a
straight lumen (i.e. the passage left between the teat-cell apices) of up to 15
μm in diameter is observed. Furthermore, as a very slight pressure exerted on a
submerged leaf provokes the emission of an air bubble through the pore and
since no mucilage filling the pore has been detected in this study, gaseous
exchanges between the atmosphere and the cavity probably remain possible.

Pore morphogenesis

On the adaxial surface of the upper lobe of the leaf primordium, a group of
epidermal cells arranged in a circle divide periclinally, giving rise to a
circular bi-layered fold (Figs. 6, 7-right). This fold limits a depression whose

epidermal cells, forming from now on the inner epidermis, enlarge periclinally (compare Figs. 6, 7-left). At the same time, the cells on the border of the bi-layered fold undergo divisions forming radially arranged rows of cells (Fig. 8). These two processes lead to the formation of a cavity that remains in contact with the atmosphere through a circular opening, or pore, with an initially almost constant mean diameter of about 60 μm, as measured at the base of its limiting cells. During this development, the bi-layered fold surrounding the pore slightly bends towards the inside of the cavity (Fig. 7-left). This invagination is due to additional anticlinal divisions of the cells from the outer layer of the fold, i.e. the adaxial epidermis. Morphological modifications then appear on the borders of the pore. Adaxial epidermal cells lining the pore elongate and become teat-shaped (Figs. 9, 10), that is: enlarged cell base, narrow cell body and rounded cell apex. Teat-cells point towards the centre of the pore, progressively reducing its lumen (Fig. 11), but never completely obstructing the passage. The basal enlargement of the teat-cells causes a more pronounced invagination of the pore borders inside the cavity, thereby leading to an increase of the pore diameter to ca. 80 μm.

Pore morphogenesis appears identical in *A. filiculoides* and *A. nilotica*. Regarding *A. pinnata* var. *pinnata*, pore morphogenesis is similar except for a few details: in this species, invagination of the pore borders towards the inner side of the cavity is barely observable if at all existent; furthermore teat-cells are arranged on only 2–3 levels. The diameter of the developing pore has the same mean value for the three species studied. In all instances this diameter slightly increases from 60 to 80 μm by the end of teat-cell differentiation.

Teat-cell ultrastructure

Transmission electron microscopy of pore teat-cells was carried out on mature, clearly not senescent leaves of *A. filiculoides*. Fronds prepared by both fixation procedures showed identical ultrastructural features. Mature teat-cells, 30–40 μm long, show an enlarged cell base of about 20 μm (Fig. 12) and are highly vacuolated. Their nucleus has a median position (Fig. 12). The cytoplasm, which is relatively homogenous in all parts of the teat-cells, has a higher organelle density than surrounding epidermal cells: mitochondria (Fig. 21), rough endoplasmic reticulum, Golgi apparatus with dilated cisternae (Fig. 13) and numerous secretion vesicles (Figs. 13, 14) are observed. The vacuole contains convoluted membrane accumulations (Fig. 15) and shows plasmalemmasomes, as described by Heath and Greenwood (1970), protruding into it (Fig. 16). Paramural bodies (Marchant and Robards, 1968) are found in the periplasm (Figs. 17–19). A great morphological diversity of these structures is observed, but two types occur more frequently. The first type

consists of spherical vesicles with a diameter up to 70 nm and containing an homogenous material slightly opaque to electrons (Fig. 17). The second type, almost exclusively located at the basis of the teat-cells, consists of larger and flattened membranous structures similar to dictyosome cisternae and is about 100 nm in length (Fig. 19). The cell wall of teat-cells, bordered by an electron dense thin layer corresponding to the cuticle (Fig. 17), is generally thinner than the cell wall of surrounding epidermal cells. Vesicles embedded in the cell wall, defined as lomasomes by Heath and Greenwood (1970), are also observed (Fig. 20). Paramural bodies and lomasomes (Figs. 17–20) cannot be interpreted as artifacts since with both fixation procedures these structures were only observed in teat-cells and never in surrounding cells. Additionally, no ultrastructural abnormalities indicative of fixation problems were observed.

In all mature pores, some teat-cells present remarkable external protuberances on their cell wall surface (Figs. 21, 22). These spherical projections, always localized near the basal part of the teat-cells, vary in number and shape. From one to more than four per teat-cell, these structures range in size from 1 to several μm in diameter. The content of the projections exhibits a very fine granular matrix that is homogeneous or heterogeneous, electron dense or transparent. Despite their variability, they present a common characteristic : they are all limited by a thin electron dense film that is in continuity with the cuticle (not visible at the magnification levels of Figs. 21 and 22). At their base thickenings of the cell wall are frequently observed (Fig. 22). Occasionally paramural bodies are also observed at their base. Such projections are never observed in any other type of cells of the upper leaf lobe.

Composition of cell wall projections

The results of cytochemical stainings are summarized in Table 1. Ruthenium Red stains the projections revealing their pectic nature (Fig. 23). The lack of reactivity with hydroxylamine/ferric chloride indicates that the pectin is not esterified. Alcian blue stains the projections positively. Gradations of reaction intensity, from weakly to strongly positive, for Alcian blue are frequently observed among teat-cell projections within a same pore. Variations of coloration, from reddish pink to deep purple-violet, are also observed with the metachromatic stain Toluidine blue (Fig. 24). Both stainings indicate the presence of acidic polysaccharides in the projections. The absence of cellulose is confirmed by the negative reaction to Calcofluor white. Aniline blue and resorcine blue mark the projections, indicating the presence of callose (Figs. 25, 26). No autofluorescence of the projections was detected, indicating the absence of lignin, suberin or cutin. The absence of lipidic compounds is demonstrated by the negative responses of the projections to Phosphine 3R and Sudan Black B.

Table 1.   Cytochemical stainings of the cell wall projections.

Stain	Specificity	Projections
Ruthenium red	Pectin	+ / ++
Hydroxylamine/ferric chloride	Esterified pectin	–
Alcian blue	Acidic polysaccharides	+ / ++
Toluidine blue	Acidic polysaccharides	purple
Calcofluor white	Cellulose	–
Aniline blue	Callose	+
Resorcine blue	Callose	+
Phosphine 3R	Lipids (- sterols)	–
Sudan black B	Total lipids	–
Coomassie brilliant blue R	Proteins	++

+: Obvious staining, ++: strong staining, –: no staining.

Coomassie Brilliant Blue R stains the teat-cell projections strongly, indicating the presence of proteins (Fig. 27).

Cell wall thickenings at the base of the projections, which may reach 3 μm, contain callose as indicated by their positive reactivity to aniline blue (Figs. 28, 29).

4. Discussion

The present study clearly established that the pore of the leaf cavity in three different species of *Azolla* subsists in fully differentiated leaves, with only limited specific morphological differences. This pore connects the cavity containing *Anabaena* and other bacteria with the external atmosphere while restricting the passage by a system of baffles formed by teat-cells originating from the adaxial epidermis of the leaf.

The very first stages of leaf development until the emergence of the epidermal fold described here correspond to those presented by Konar and Kapoor (1972). These authors, as well as Demalsy (1953), had nevertheless concluded a progressive, even if partial, closure of the pore during later developmental stages, through proliferation of the cells bordering it. Our observations demonstrate that it is not the proliferation of these cells but only their elongation into teat-shaped unicellular trichomes which protrude into the lumen that partially obstruct the pore. Actually its total diameter, as defined in this study, slightly increases at the end of leaf development. A

total closure of the cavity as referred by some authors (Smith, 1955; Calvert and Peters, 1981; Becking, 1987) was never observed in any of the three *Azolla* species investigated in this study.

The subsistence of a pore connecting the leaf cavity with the external environment and the apparent absence of mucilage in this pore implies the possibility of gaseous exchanges between these two compartments. The lower oxygen concentration in the leaf cavities than in the atmosphere reported by Grilli Caiola et al. (1989) and Uheda et al. (1995) do not imply an obstruction of the pore by mucilage. These observations can be explained by considering the cavity as a metabolically active and very confined, although open, compartment. Nevertheless, further evidences – such as could be provided by a LTSEM study – are needed to confirm definitively the absence of mucilagineous material in the pore region. The morphology of the teat-cells, forming a system of baffles, suggests their possible function as a mechanical filter, preventing particles and organisms from entering and the *Anabaena* colony from exiting.

Moreover, TEM observations suggest a second function for the teat-cells, namely a secretory role. The occurrence of a high density of organelles and ribosomes and of numerous secretion vesicles and abundant membranous profiles is indicative of a high metabolic activity. Paramural bodies in the periplasm suggest a secretory activity (Moore and McAlear, 1961; Marchant and Robards, 1968; Roland, 1973; Gram, 1982) as does the protrusion of plasmalemmasomes into the vacuole; Heath and Greenwood (1970) suggested indeed that membrane excess resulting from fusions of numerous secretion vesicles with the plasmalemma (Juniper et al., 1981) or from the accumulation of paramural bodies in the periplasm, is transferred to the vacuole for disaggregation. A similar explanation may account for the accumulation of convoluted membranes in the vacuole.

The very existence of cell wall projections also supports the hypothesis of a secretory function for teat-cells. Cytochemical tests showed that the projections are composed of a mixture of unesterified pectin, callose and proteins. Morphologically similar projections have repeatedly been reported in the literature (Carlquist, 1956; Davies and Lewis, 1981; Donaldson and Singh, 1984; Jeffree et al., 1989; Suske and Acker, 1989; Read, 1990; Scheidegger et al., 1991; Miller and Barnett, 1993; Günthardt-Goerg et al., 1997) but were never found on epidermal cells. Although these reported structures vary in composition, the presence of pectin has generally been demonstrated. These projections were described to appear under stress situations such as wounding (Davies and Lewis, 1981), grafting (Jeffree et al., 1989; Miller and Barnett, 1993), fungal infection (Suske and Acker, 1989; Read, 1990; Scheidegger et al., 1991) and ozone exposure (Scheidegger et al., 1991; Günthardt-Goerg et al., 1997). In our culture conditions however no sign of stress was ever noticed. The

secretory nature of the teat-cells, as shown here, and the cell wall projections may suggest a preemptive chemical defence against invading organisms. Davies and Lewis (1981), observing projections on wound callus cells of *Daucus carota*, suggested that they contribute to the elaboration of a water-proof barrier on the cell surface to prevent dehydration. Besides the obvious morphological similarity between the projections they observed and those occurring on teat-cells of *Azolla*, the callus cells bearing projections also presented convoluted membranous structures and multivesicular bodies that may indicate processes of projection formation similar in both carrot and *Azolla*. Despite the absence of lipidic compounds, projections of the *Azolla* teat-cells could indeed be associated with non-wettability preventing the ingress of water by capillarity into the leaf cavity because the possible water-repellent effect of the proteins detected in the projections (Gerin et al., 1993; Beever et al., 1979).

Further studies are in progress to establish the kinetics of the differentiation of teat-cells and the role of the pore and its surrounding associated cells in the *Azolla-Anabaena* symbiosis.

Acknowledgements

REFERENCES

Becking, J.H. 1987. Endophyte transmission and activity in the *Anabaena-Azolla* association. *Plant and Soil* **100**: 183–212.

Beever, R.E., Redgwell, R.J., and Dempsey, G.P. 1979. Purification and chemical characterization of the rodlet layer of *Neurospora crassa* conidia. *Journal of Bacteriology* **140**: 1063–1070.

Calvert, H.E. and Peters, G.A. 1981. The *Azolla-Anabaena azollae* relationship. IX. Morphological analysis of leaf cavity hair populations. *New Phytologist* **89**: 327–335.

Calvert, H.E., Pence, M.K., and Peters, G.A. 1985. Ultrastructural ontogeny of leaf cavity trichomes in *Azolla* implies a functional role in metabolite exchange. *Protoplasma* **129**: 10–27.

Carlquist, S. 1956. On the occurrence of intercellular pectic warts in Compositae. *American Journal of Botany* **43**: 425–429.

Davies, W.P. and Lewis, B.G. 1981. Development of pectic projections on the surface of wound callus cells of *Daucus carota* L. *Annals of Botany* **47**: 409–413.

Demalsy, P. 1953. Etudes sur les hydropteridales. III. Le sporophyte d'*Azolla nilotica*. *Cellule* **56**: 7–60.

1

Donaldson, L.A. and Singh, A.P. 1984. Cell wall protuberances in the resin-pocket callus of *Pinus nigra*. *Canadian Journal of Botany* **62**: 570–574.

Fisher, D.B. 1968. Protein staining of ribboned epon sections for light microscopy. *Histochemie* **16**: 92–96.

Gerin, P.A., Dufrene, Y., Bellon-Fontaine, M.N., Asther, M., and Rouxhet, P.G. 1993. Surface properties of the conidiospores of *Phanerochaete chrysosporium* and their relevance to pellet formation. *Journal of Bacteriology* **175**: 5135–5144.

Gram, N.H. 1982. The ultrastructure of germinating barley seeds. 1. Changes in the scutellum and the aleurone layer in barley *Hordeum vulgare* cultivar Nordal. *Carlsberg Research Communications* **47**: 143–162.

Grilli Caiola, M., Canini, A., and Moscone, D. 1989. Oxygen concentration, nitrogenase activity and heterocyst frequency in the leaf cavities of *Azolla filiculoides* Lam. *FEMS Microbiology Letters* **59**: 283–288.

Günthardt-Goerg, M.S., McQuattie, C.J., Scheidegger, C., Rhiner, C., and Matyssek, R. 1997. Ozone-induced cytochemical and ultrastructural changes in leaf mesophyll cell walls. *Canadian Journal of Forest Research* **27**: 453–463.

Heath, I.B. and Greenwood, A.D. 1970. The structure and formation of lomasomes. *Journal of General Microbiology* **62**: 129–137.

Jeffree, C.E., Gordon, F., and Yeoman, M.M. 1989. Pectinaceous beads and pectinase on callus cell surfaces in graft unions and in culture. In: *Cell Separation in Plants*. D.J. Osborne and M.B. Jackson, eds. NATO ASI Series vol. H 35, Springer-Verlag, Berlin, pp. 287–299.

Jensen, W.A. 1962. *Botanical Histochemistry*. Freeman and Co., San Francisco and London.

Juniper, B.E., Lawton, J.R., and Harris, P.J. 1981. Cellular organelles and cell-wall formation in fibres from the flowering stem of *Lolium temulentum* L. *New Phytologist* **89**: 609–619.

Komárek, J. and Anagnostidis, K. 1989. Modern approach to the classification system of cyanophytes. IV. Nostocales. *Archives of Hydrobiology*. Suppl. 82. Algological Studies **56**: 301–345.

Konar, R.N. and Kapoor, R.K. 1972. Anatomical studies on *Azolla pinnata*. *Phytomorphology* **22**: 211–223.

Letham, D.S. 1960. The separation of plant cells with ethylenediaminetetraacetic acid. *Experimental Cell Research* **21**: 353–360.

Marchant, R. and Robards, A.W. 1968. Membrane systems associated with the plasmalemma of plant cells. *Annals of Botany* **32**: 457–471.

Meeks, J.C., Joseph, C.M., and Haselkorn, R. 1988. Organization of the nif genes in cyanobacteria in symbiotic association with *Azolla* and *Anthoceros*. *Archives of Microbiology* **150**: 61–71.

Miller, H. and Barnett, J.R. 1993. The structure and composition of bead-like projections on Sitka spruce callus cells formed during grafting and in culture. *Annals of Botany* **72**: 441–448.

Moore, R.T. and McAlear, J.H. 1961. Fine structure of mycota. V. Lomasomes – previously uncharacterized hyphal structures. *Mycologia* **53**: 194–200.

Nierzwicki-Bauer, S.A. and Aulfinger, H. 1991. Occurrence and ultrastructural characterization of bacteria in association with and isolated from *Azolla caroliniana*.

Applied and Environmental Microbiology **57**: 3629–3636.

Peters, G.A. and Meeks, J.C. 1989. The *Azolla-Anabaena* symbiosis: basic biology. *Annual Reviews of Plant Physiology* **40**: 193–210.

Peters, G.A., Toia, R.E.Jr., Raveed, D., and Levine, N.J. 1978. The *Azolla-Anabaena azollae* relationship. VI. Morphological aspects of the association. *New Phytologist* **80**: 583–593.

Popper, H. 1944. Distribution of vitamin A in tissue as visualized by fluorescence microscopy. *Physiological Reviews* **24**: 205–224.

Rao, H.S. 1935. The structure and life-history of *Azolla pinnata* R. Brown with remarks on the fossil history of the Hydropterideae. *Proceedings of the Indian Academy of Science* **2**: 175–208.

Read, N.D. 1990. Low temperature scanning electron microscopy of fungi and fungus-plant interactions. In: *Electron Microscopy of Plant Pathogens*. K. Mendgen and D.E. Lesemann, eds. Springer-Verlag, Berlin, pp. 17–29.

Reeve, R.M. 1959. A specific hydroxylamine-ferric chloride reaction for histochemical localization of pectin. *Stain Technology* **34**: 209–211.

Reynolds, E.S. 1963. The use of lead citrate at high pH as an electron opaque stain in electron microscopy. *Journal of Cell Biology* **17**: 208–212.

Roland, J.C. 1973. The relationship between the plasmalemma and plant cell wall. *International Review of Cytology* **36**: 45–84.

Roland, J.C. and Vian, B. 1991. General preparation and staining of thin sections. In: *Electron Microscopy of Plant Cells*. J.L. Hall and C. Hawes, eds. Academic Press, London, pp. 1–66.

Schaede, R. 1947. Untersuchungen über *Azolla* und ihre Symbiose mit Blaualgen. *Planta* **35**: 319–330.

Scheidegger, C., Günthardt-Goerg, M.S., Matyssek, R., and Hatvani, P. 1991. Low-temperature scanning electron microscopy of birch leaves after exposure to ozone. *Journal of Microscopy* **161**: 85–95.

Smith, G.M. 1955. *Cryptogamic Botany. Vol. II: Bryophytes and Pteridophytes*. McGraw-Hill, New York.

Spurr, A.R. 1969. A low viscosity epoxy resin embedding medium for electron microscopy. *Journal of Ultrastructure Research* **26**: 31–43.

Strasburger, E. 1873. *Ueber Azolla*. Hermann Dabis, Jena.

Suske, J. and Acker, G. 1989. Identification of endophytic hyphae of *Lophodermium piceae* in tissues of green, symptomless Norway spruce needles by immunoelectron microscopy. *Canadian Journal of Botany* **67**: 1768–1774.

Uheda, E., Kitoh, S., Dohmaru, T., and Shiomi, N. 1995. Isolation and analysis of gas bubbles in the cavities of *Azolla* leaves. *Physiologia Plantarum* **93**: 1–4.

Van Coppenolle, B., Watanabe, I., Van Hove, C., and McCouch, S.R. 1993. Genetic diversity and phylogeny analysis of *Azolla* based on DNA amplification by arbitrary primers. *Genome* **36**: 686–693.

Van Hove, C., de Waha Baillonville, T., Diara, H.F., Godard, P., Mai Kodomi, Y., and Sanginga, N. 1987. *Azolla* collection and selection. In: *Azolla Utilization*. International Rice Research Institute, Los Baños, pp. 77–87.